https://doi.org/10.5194/egusphere-2025-3796
Preprint. Discussion started: 27 August 2025

Measurement report: Dust impact on hygroscopicity and volatility of submicron aerosols: Based on the observation in April of Beijing

Xinyao Hu[1,2], Aoyuan Yu[1,3], Xiaojing Shen[1,2], Jiayuan Lu[1,4], Yangmei Zhang[1,2], Quan Liu[1,2], Lei Liu[1,2], Linlin Liang[1,2], Hongfei Tong[1,2], Qianli Ma[5], Shuxian Zhang[5], Bing Qi[6], Rongguang Du[6], Huizheng Che[1,2], Xiaoye Zhang[1,2], and Junying Sun[1,2*]

[1]State Key Laboratory of Severe Weather Meteorological Science and Technology, Chinese Academy of Meteorological Sciences, Beijing, 100081, China
[2]Key Laboratory of Atmospheric Chemistry of CMA, Chinese Academy of Meteorological Sciences, Beijing, 100081, China
[3]Dalian Meteorological Observatory, Dalian, 116000, China
[4]Department of Atmospheric and Oceanic Sciences and Institute of Atmospheric Sciences, Fudan University, Shanghai, 200433, China
[5]Lin'an Atmosphere Background National Observation and Research Station, Lin'an 311307, Hangzhou, China
[6] Hangzhou Meteorological Bureau, Hangzhou, 310051, China
*Correspondence to: Junying Sun (jysun@cma.gov.cn)

Abstract.

Understanding the aerosol hygroscopicity and volatility is crucial for determining their effects on the environment and climate. As a typical natural aerosol, the dust impact on fine particles' hygroscopicity and volatility remains inadequately understood. Simultaneous measurements of aerosol hygroscopicity and volatility were performed using Volatility-Hygroscopicity Tandem Differential Mobility Analyzer during April 2024 in Beijing. During this period, mean hygroscopic growth factor (HGF) of 50, 80, 110, 150, 200, and 300 nm were 1.20±0.07, 1.28±0.07, 1.32±0.07, 1.36±0.08, 1.40±0.09, and 1.43±0.13, respectively. The mean volatile shrink factor (VSF) was

https://doi.org/10.5194/egusphere-2025-3796
Preprint. Discussion started: 27 August 2025

0.48±0.05, 0.52±0.04, 0.53±0.05, 0.53±0.06, 0.53±0.07, and 0.54±0.10. Particles from anthropogenic emissions were dominated by more hygroscopic and volatile components, while particles influenced by natural sources (such as dust) had lower hygroscopicity and volatility. The case study highlighted the impact of dust on hygroscopicity and volatility for accumulated mode particles. Before dust arrival, more hygroscopic and very volatile mode were more prominent, and HGF increased and VSF decreased with diameter. When dust arrived, the number fraction of more hygroscopic mode (NF_{MH}) dropped to 0.54 (200 nm) and 0.33 (300 nm), while number fraction of very volatile mode (NF_{VV}) fell to 0.73 (200 nm) and 0.47 (300 nm), respectively. This reflected a shift toward the hydrophobic and non-volatile components. During dust period, the size dependence showed that HGF peaked at 150 nm and declined, whereas VSF rose with diameter. The mean HGF and VSF at 300 nm were 1.20 and 0.74 during dust period, suggesting that particles at 300 nm were hydrophobic and less volatile.

1. Introduction

Hygroscopicity and volatility are critical physical properties of atmospheric aerosol particles. Hygroscopicity has a significant influence on atmospheric radiative balance and visibility by altering particle size distribution and optical properties. In addition, hygroscopicity indirectly affects the regional and global climate by influencing the lifetime and microphysical properties of clouds (Gunthe et al., 2009; Rose et al., 2010; Pöhlker et al., 2023). Volatility plays a crucial role in gas-particle partitioning and the aging process of aerosols (Huffman et al., 2008). Considering the hygroscopicity and volatility of aerosols in the model is of great significance for reducing discrepancies between simulation results and observational data, and improving the accuracy of model outputs (Gao et al., 2024; Mcfiggans et al., 2006; Pringle et al., 2010; Rissler et al., 2010). Besides, determining the variation of particle size at selected dry diameters under different relative humidity and temperatures can also provide valuable indirect in-situ information regarding the chemical composition, mixing state, and coating properties of aerosols (Massoli et al., 2010; Chen et al., 2022a;

https://doi.org/10.5194/egusphere-2025-3796
Preprint. Discussion started: 27 August 2025

Liu et al., 2025).

Given the significant environmental and climatic effects of aerosol volatility and hygroscopicity, numerous field observations on aerosol volatility or hygroscopicity have been conducted. Previous researches show that the volatility and hygroscopicity of fine particles exhibit substantial differences due to the influence of emission sources and atmospheric processes. The observed results in five sites across China by Chen et al. (2022b) demonstrated that aerosols at suburban sites were more hygroscopic than those in megacities, which may be attributed to the fact that suburban aerosols were mainly from regional transport and thus more aged and well mixed. Cai et al. (2017) found that aerosols exhibited lower volatility in Guangzhou compared to Okinawa, because the aerosols in Guangzhou were affected more by traffic-related sources and industrial emissions.

The size dependence of hygroscopicity and volatility is complex. Wu et al. (2016) demonstrated a clear increasing trend in hygroscopicity with particle size, which was similar to the size dependency of inorganic mass fraction in PM_1. While Shi et al. (2022) found that aerosol hygroscopicity for 60, 100, 150, and 200 nm at 90% RH in rural North China decreases with increasing particle size in winter, possibly due to enhanced domestic heating emissions of non-hygroscopic or low-hygroscopicity primary aerosols under low temperatures. In terms of volatility, the VSF of ambient aerosols in urban Beijing decreases with increasing particle size (Wang et al., 2017), while Levy et al. (2014) reported the opposite size dependence near the California-Mexico border. Besides, the size dependence of volatility various under different pollution conditions. Yu et al. (2025) found that volatility declined slightly with particle size under the clean conditions, without an obvious size dependence under the pollution conditions.

Dust particles, suspended in the atmosphere, range from less than 0.1μm to over 100μm (Adebiyi et al., 2023). As one of the most important natural aerosols in the atmosphere, dust aerosols significantly affect atmospheric chemistry, human health, climate change, and biogeochemical cycles (Chen et al., 2021; Kurai et al., 2014; Lian et al., 2025). Heterogeneous reactions between mineral dust and trace gases can alter

https://doi.org/10.5194/egusphere-2025-3796
Preprint. Discussion started: 27 August 2025

the chemical and physical properties of aerosols (Tang et al., 2017; Xu et al., 2020; Kok et al., 2023). Although the climatic and environmental effects of dust are considerable, limited studies focus on the dust effect on aerosol hygroscopicity and volatility simultaneously, especially on submicron aerosols (Kaaden et al., 2009; Kim and Park, 2012; Massling et al., 2007).

The North China Plain (NCP) is a hot spot of anthropogenic emissions, which can lead to severe air pollution. In recent years, the air quality in the NCP has significantly improved due to the strict control measures implemented by the government. However, the air pollution still happens due to unfavorable meteorological conditions, particularly in spring (Hu et al., 2021; Zhong et al., 2021). On the other hand, dust events often occur in the NCP in spring (Gui et al., 2023; Gui et al., 2022), which complicates the characteristics of aerosol hygroscopicity and volatility of the NCP. Although aerosol hygroscopicity and volatility in the North China Plain have been widely discussed in previous studies, existing work primarily focuses on the impact of chemical composition on aerosol hygroscopicity and volatility, the influence of anthropogenic emission on the hygroscopicity and volatility of aerosols, and the characterization of aerosol hygroscopicity and volatility under different pollution conditions(Wu et al., 2016; Chen et al., 2022a; Chen et al., 2022b; Shi et al., 2022; Zhang et al., 2023; Yu et al., 2025). The understanding of aerosol hygroscopicity and volatility in spring, particularly during the dust period, is limited.

In this study, the hygroscopicity and volatility of aerosols were measured simultaneously using a Volatility-Hygroscopicity Tandem Differential Mobility Analyzer (VH-TDMA) in the spring of 2024. The characteristics of aerosol hygroscopicity and volatility were analyzed, and the influence of air mass on aerosol hygroscopicity and volatility was discussed. Moreover, the relationships between hygroscopicity and volatility were explored. Finally, the impact of dust on the hygroscopicity and volatility of aerosol was investigated through a case study of a dust event. The study aimed to enhance understanding of aerosol hygroscopicity and volatility in spring, and to reveal the dust effect on the hygroscopicity and volatility of

https://doi.org/10.5194/egusphere-2025-3796
Preprint. Discussion started: 27 August 2025

fine particles.

2. Experiment and instrumentation

2.1 Sampling site

The measurements were performed at the Chinese Academy of Meteorological Sciences (CAMS; 39.97°N, 116.37°E) from April 1st to April 29th, 2024. The CAMS site is a typical urban site between the second-ring and third-ring roads in Beijing. There is a major road within 200 meters to the west of the CAMS site. Local residents and traffic emissions are the major sources of emissions at the CAMS site. More details about the CAMS site are provided in the following studies(Zhang et al., 2023; Lu et al., 2024).

2.2 Instrumentation

2.2.1 Aerosol hygroscopicity and volatility measurement

The size-resolved aerosol hygroscopicity and volatility were measured by a Volatility Hygroscopicity Tandem Differential Mobility Analyzer (VH-TDMA) (TROPOS, Germany), which is described in detail by Yu et al. (2025). Here, we just introduced briefly. The sample air was dried by a silica dryer and a Nafion dryer to keep its RH<30% before being pumped into the VH-TDMA. The VH-TDMA is composed of an X-ray aerosol neutralizer (model 3088, TSI Inc., USA), two condensation particle counters (CPC1 and CPC2; CPC 3772, TSI Inc., USA), and three medium Hauke-type differential mobility analyzers (DMA1, DMA2, and DMA3, TROPOS, Germany), custom-made Nafion dryers, thermal denuders (TDs), and humidifiers.

In this study, the VH-TDMA operates alternately in the H-TDMA mode and the V-TDMA mode, which can measure the aerosol hygroscopicity and volatility simultaneously. DMA1 selected quasi-monodisperse particles at selected diameters (Dp = 50, 80, 110, 150, 200, and 300 nm). Then the aerosol particles of a certain size were split into two flows. One flow passed through the TDs, followed by DMA2 and CPC1,

https://doi.org/10.5194/egusphere-2025-3796
Preprint. Discussion started: 27 August 2025

and the other flow passed through the humidifiers, and DMA3+CPC2. DMA2+CPC1 measured the size distribution of heated particles and DMA3+CPC2 measured the size distribution of humidified particles, respectively. In this study, the temperature in the TDs was set at 300 °C and the RH in the humidifier was set at 90%. In order to ensure the accuracy of the RH measurement, the hygroscopicity of 100 nm ammonium sulfate particles was measured regularly during the campaign. In this study, we used the TDMAinv program package (Gysel et al., 2009) to inverted the data from VH-TDMA.

2.2.2 Particle number size distribution measurement

The particle number size distribution (PNSD) in the range of 8-850 nm under dry conditions (RH<30%) was measured in spring of 2024 (including dust period) by a tandem scanning mobility particle sizer (TSMPS, TROPOS, Germany). The TSMPS consists of two differential mobility analyzers (DMAs, TROPOS, Germany) and two condensation particle counters (CPCs, models 3772 and 3776, TSI Inc., St Paul, USA). More information on PNSD measurement and setup is described in (Shen et al., 2018).

2.3 Data processing

The hygroscopic growth factor (HGF) is defined as the ratio of the particle's electrical mobility diameter at a certain relative humidity to that under dry conditions:

$$\mathrm{HGF} = \frac{Dp(wet)}{Dp_{(dry,T0)}}$$

Where Dp(wet) is the particle diameter at an RH of 90%, Dp(dry,T0) refers to the particle diameter at room temperature with an RH below 30%.

The volatile shrink factor (VSF) is defined as the ratio of the particle's electrical mobility diameter at a certain temperature to that under dry conditions at room temperature:

$$\mathrm{VSF} = \frac{Dp(T1)}{Dp_{(dry,T0)}}$$

Where Dp(T1) is the particle diameter at a set heating temperature of 300°C.

The hygroscopic growth factor probability density function (HGF-PDF) and volatile shrink factor probability density function (VSF-PDF) were derived from the

https://doi.org/10.5194/egusphere-2025-3796
Preprint. Discussion started: 27 August 2025

number size distributions of humidified aerosol particles and volatile aerosol particles. According to the HGF-PDF, aerosol particles were divided into two hygroscopic groups: nearly hydrophobic (NH) mode particles (HGF $\leq$ 1.2) and more hygroscopic (MH) mode particles (HGF > 1.2). Based on the VSF-PDF, aerosol particles were classified into two groups: non-volatile (NV) mode particles (VSF $\geq$ 0.8) and very volatile (VV) mode particles (VSF < 0.8). The detailed description of the calculation methods for HGF-PDF, VSF-PDF, and the number fraction (NF) of each mode was shown in Yu et al. (2025)

2.4 Other data used

Hourly $PM_{2.5}$ and PM_{10} mass concentrations at the Guanyuan site were obtained from the China National Environmental Monitoring Center. The meteorological data at Haidian station (No.54399), which is located 5 km northwest of the CAMS site, was obtained from the National Meteorological Information Center of the China Meteorological Administration. Besides, the 48-hour back trajectories arriving at the CAMS site were calculated using the HYSPLIT 4 model (Hybrid Single-Particle Lagrangian Integrated Trajectory)(Draxler and Hess, 1998; Cohen et al., 2015). All data in this study are reported in Beijing time (UTC+8).

https://doi.org/10.5194/egusphere-2025-3796
Preprint. Discussion started: 27 August 2025

3. Results and discussion

3.1 Overview

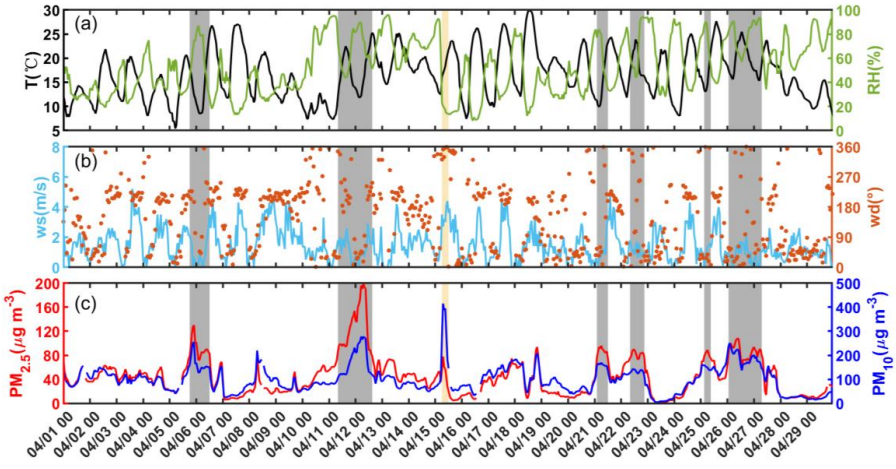

Figure 1. Time series of temperature and relative humidity (a), wind speed and wind direction (b), $PM_{2.5}$ and PM_{10} mass concentration (c) from April 1 to 29, 2024. The gray-shade and yellow-shade area represent the pollution period and dust period, respectively.

The time series of meteorological parameters and $PM_{2.5}$ and PM_{10} mass concentrations are depicted in Figure 1. During the study period, the average temperature was 16.6±5.1 ℃ and the mean RH was 53.2±23.1%. The average wind speed was 1.48 ±1.06 m/s, with the highest value up to 5.2 m/s. The mean $PM_{2.5}$ and PM_{10} mass concentrations were 44.9±32.3 and 100.7±57.0 μg/m^3 during the study period. There were six pollution episodes and one dust episode during the whole campaign. Here, the pollution episode was defined as the $PM_{2.5}$ mass concentration exceeding 75 μg/m^3 and the ratio of $PM_{2.5}$ and PM_{10} exceeding 0.3. Dust episode was defined as the PM_{10} mass concentration was larger than 100 μg/m^3 and the ratio of $PM_{2.5}$ and PM_{10} was smaller than 0.3. During the pollution period, southerly winds prevailed with low wind speed and high relative humidity. When dust arrived, the prevailing wind is usually from the northwest with high wind speed with low RH.

https://doi.org/10.5194/egusphere-2025-3796
Preprint. Discussion started: 27 August 2025

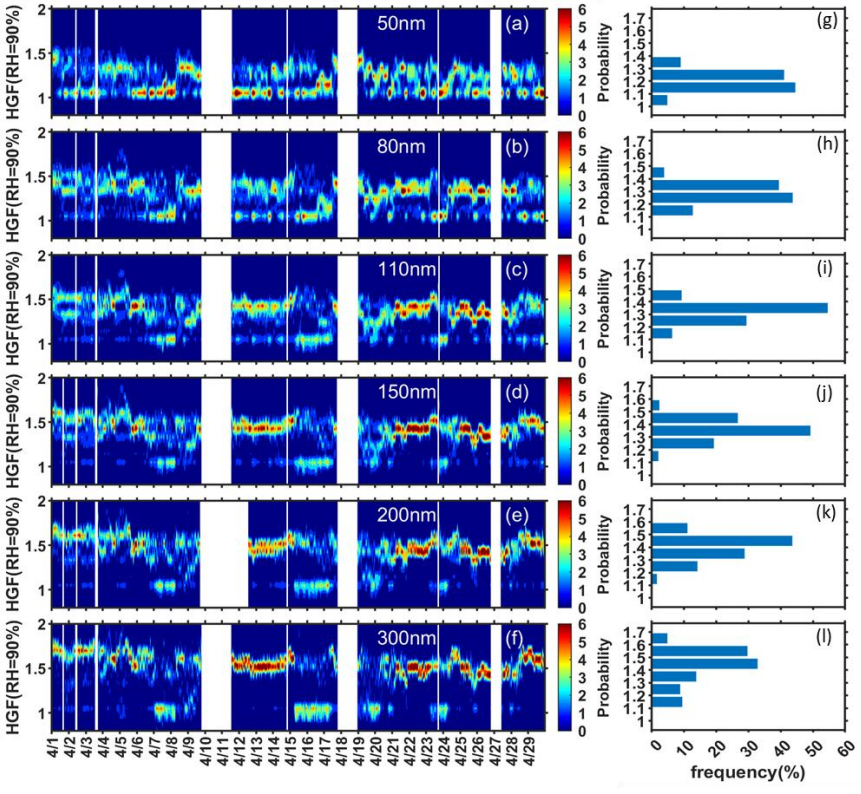

Figure 2. Time series of HGF-PDFs for 50, 80, 110, 150, 200 and 300 nm particles at 90% RH (a–f), and the frequency of the HGF values (g–l).

In this study the minimum HGF-PDF for 50, 80, 110, 150, 200 and 300 nm particles are typically at around 1.2 (Figure. S1), so the particles are divided into two modes: the nearly hydrophobic (NH) mode particles (HGF < 1.2) and more hygroscopic (MH) mode particles (HGF > 1.2). Figure 2 displays the time series of HGF-PDFs for 50, 80, 110, 150, 200 and 300 nm particles at 90% RH and the frequency of the HGF values. During the study period, the HGF for 50 nm particles was dominated by the NH mode, with the highest frequency of HGF ranging from 1.1 to 1.2. This could be related to the particles for 50nm, mainly influenced by local emission, such as traffic emissions. For 80, 110, 150, 200, and 300 nm particles, the MH mode in the HGF-PDF was basically more dominant. HGFs for 80 and 110 nm particles were mainly distributed between 1.2 and 1.3. For 150 and 200 nm particles, HGF mainly ranged from 1.3 to 1.4.

https://doi.org/10.5194/egusphere-2025-3796
Preprint. Discussion started: 27 August 2025

The distribution range of HGF for 300nm particles was wider, primarily ranging from 1.4 to 1.6. During the whole period, the number fraction of more hygroscopic mode particles (NF_{MH}) for 50, 80, 110, 150, 200, and 300 nm particles was 51%, 68%, 75%, 79%, 80%, 77%, respectively. Only half of the particles at 50 nm were more hygroscopic, which was due to the intensive emissions from traffic and cooking sources around the site. The CAMS site is surrounded by residents and is near the main road with heavy traffic. The particles from traffic and cooking sources are usually externally mixed and hydrophobic(Henning et al., 2010). The NH mode was hardly observed in aerosol particles ranging from 150 to 300nm during the pollution period, indicating the particles were almost hygroscopic and more aged (Zhang et al., 2023). As shown in Table 1, HGF shows a strong size dependency. The mean values of HGF for 50 - 300nm particles were 1.20±0.07, 1.28±0.07, 1.32±0.07, 1.36±0.08, 1.40±0.09, 1.43±0.13, which were consistent with the results observed by Wang et al. (2017) that aerosol particles became more hygroscopic with increasing particle size.

https://doi.org/10.5194/egusphere-2025-3796
Preprint. Discussion started: 27 August 2025

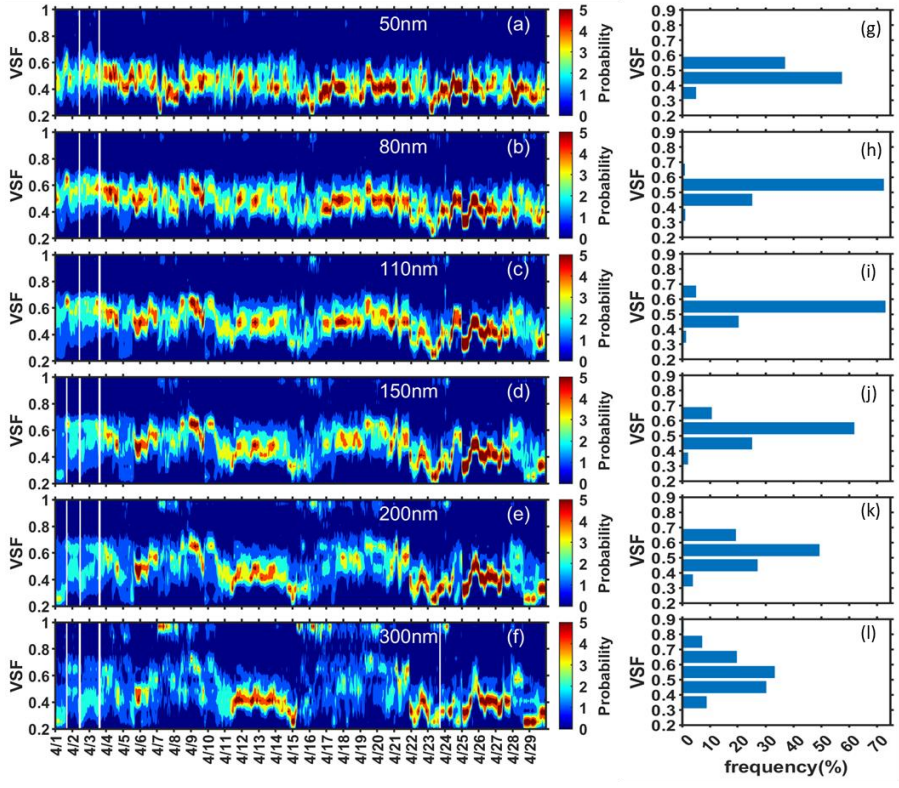

Figure 3. Time series of VSF-PDF for 50, 80, 110, 150, 200 and 300 nm particles (a–f), and the frequency of the VSF values (g–l).

After the aerosol is heated to 300℃, the remaining substances are non-volatile substances, such as elemental carbon and dust. As shown in Figure S1, the mean VSF-PDFs show a minimum value at around 0.8, and the particles are separated into two modes: the non-volatile (NV) mode particles (VSF > 0.8) and the very volatile (VV) mode particles (VSF ≤ 0.8). Figure 3 shows the variation of volatile shrink factor probability density functions (VSF-PDFs) and the frequency distribution of VSF for 50, 80, 110, 150, 200 and 300 nm particles. The VSF-PDFs for particles in the 50-300 nm range were mainly dominated by the VV mode, with occasional enhancement of the NV mode for particles at 200, and 300 nm. During the sampling period, the mean number fraction of very volatile mode particles (NF_{VV}) for 50, 80, 110, 150, 200 and 300 nm particles was 96%, 95%, 94%, 93%, 91%, 87%, respectively, indicating the

https://doi.org/10.5194/egusphere-2025-3796
Preprint. Discussion started: 27 August 2025

particles were almost volatile. VSF for 50 -150nm particles was mainly concentrated in the range between 0.4 and 0.6. The distribution range of VSF for 300nm particles was wider, suggesting that the volatility of 300 nm aerosol particles varied greatly. During the study period, the mean value of VSF for 50 - 300nm particles was 0.48±0.05, 0.52 ±0.04, 0.53±0.05, 0.53±0.06, 0.53±0.07, 0.54±0.10, respectively.

Table 1. The hygroscopicity an volatility parameter during the campaign.

		50nm	80nm	110nm	150nm	200nm	300nm
Total	NF_{MH}	0.51±0.21	0.68±0.17	0.75±0.15	0.79±0.14	0.80±0.16	0.77±0.22
	HGF	1.20±0.07	1.28±0.07	1.32±0.07	1.36±0.08	1.40±0.09	1.43±0.13
	NF_{VV}	0.96±0.04	0.95±0.04	0.94±0.05	0.93±0.05	0.91±0.07	0.87±0.12
	VSF	0.48±0.05	0.52±0.04	0.53±0.05	0.53±0.06	0.53±0.07	0.54±0.10
Dust	NF_{MH}	0.44±0.11	0.50±0.15	0.57±0.13	0.62±0.08	0.54±0.08	0.33±0.15
	HGF	1.20±0.04	1.26±0.07	1.30±0.06	1.34±0.05	1.31±0.05	1.20±0.08
	NF_{VV}	0.93±0.05	0.89±0.04	0.87±0.04	0.83±0.04	0.73±0.09	0.47±0.21
	VSF	0.46±0.04	0.51±0.02	0.52±0.02	0.53±0.02	0.57±0.03	0.74±0.12

3.2 Influence of air mass on aerosol hygroscopicity and volatility

The hygroscopicity and volatility of aerosols are closely related to the source of air masses (Cai et al., 2017). The chemical components, aging degrees, and mixing states of aerosols carried by air masses originating from different regions are different, which leads to significant differences in the properties of aerosols corresponding to different air masses. In order to investigate the influence of air mass on aerosol hygroscopicity and volatility. The 48-h back trajectories were calculated, and the back trajectories were classified into four clusters. As shown in Figure 4, cluster 1 originated from the Bohai Sea, passed through Tianjin, and reached Beijing, which accounted for 27% of the total back trajectories. Cluster 2 originated from Mongolia, and had the longest transport distance. Cluster 2 arrived in Beijing through Inner Mongolia and the northwest of Hebei province. Cluster 3, which accounted for 39% of total back trajectories, arrived in Beijing from the Shanxi province and southwest of Hebei province. Cluster 4 originated from the northeast of Inner Mongolia and passed through

https://doi.org/10.5194/egusphere-2025-3796
Preprint. Discussion started: 27 August 2025

the Liaoning Province and the northeast of Hebei Province. The HGF corresponding to Cluster 1 was significantly greater than that of the other clusters. This might be related to the fact that Cluster 1 passed through the Bohai Sea during its transport, carrying more hygroscopic marine aerosols. The HGF of cluster 1 at 150 nm is 1.41, which is close to the result of ambient marine aerosol particles at 145nm (Hakala et al., 2016). Cluster 2, which originated from the northwest, had a smaller HGF and a larger VSF, suggesting that the particles from the northwestern air mass had weak hygroscopicity and weak volatility. This is because Cluster 2 passed through the Gobi Desert during its transport, carrying dust aerosols, which led to a decrease in the aerosol hygroscopicity and volatility.

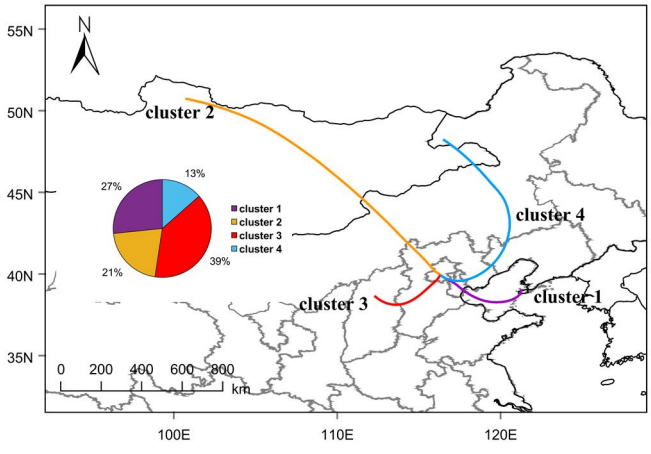

Figure 4. Air mass clusters of 48-h back trajectories arriving at the CAMS site in Beijing during the study period, and the fraction of each cluster accounting for the total back trajectories.

https://doi.org/10.5194/egusphere-2025-3796
Preprint. Discussion started: 27 August 2025

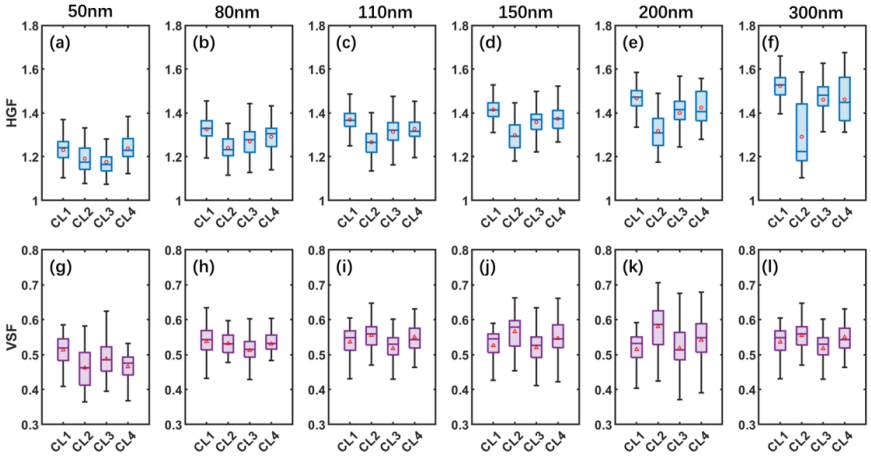

Figure 5. The variation of size- resolved HGF (a-f) and VSF (g-l) in each cluster in the campaign. The solid line in the box represents the median value, and the dot indicates the mean value. The box contains the range of values from 25 % (bottom) to 75 % (top), and the upper and lower whiskers are the 95th and 5th percentiles, respectively.

https://doi.org/10.5194/egusphere-2025-3796
Preprint. Discussion started: 27 August 2025

3.3 Relationship between aerosol hygroscopicity and volatility

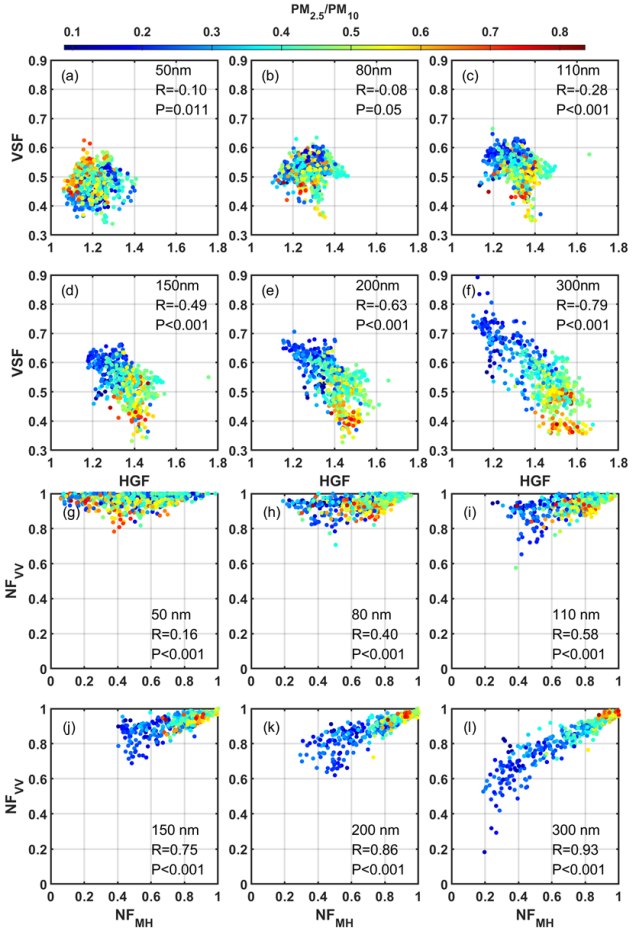

Figure 6. The relationship between HGF and VSF (a-f), as well as NF_{VV} and NF_{MH} (g-l). Color bar represents the mass ratio of $PM_{2.5}$ and PM_{10}.

In order to explore the relationships between aerosol hygroscopicity and volatility, the relationships between HGF and VSF, as well as NF_{VV} and NF_{MH}, were analyzed. Figure 6 exhibits the relationship between HGF and VSF, as well as NF_{VV} and NF_{MH}. During the observation period, there was no significant correlation between the HGF and VSF of the 50nm and 80nm aerosol particles, and the correlations between the NF_{VV} and NF_{MH} of the 50nm and 80nm aerosol particles were relatively weak. Previous studies in Beijing also found similar results, which might be related to the low degree of ageing in Aitken mode particles (Wang et al., 2017). The accumulation mode

https://doi.org/10.5194/egusphere-2025-3796
Preprint. Discussion started: 27 August 2025

particles exhibited a significant negative correlation between HGF and VSF, and the correlation became strong with increasing particle size. The relationship between hygroscopicity and volatility of accumulation mode particles was different from that of Aitken mode particles, which could be related to the aerosol chemical composition. Previous studies in Beijing revealed that the particles below 100nm are mainly organics (Li et al., 2023), while accumulation mode particles are dominated by secondary aerosols (Xu et al., 2015).

The color bar in Figure 6 represents the ratio of $PM_{2.5}$ to PM_{10}, which is used to distinguish anthropogenic pollution from dust episodes (Querol et al., 2001). A higher $PM_{2.5}/PM_{10}$ ratio usually indicates that fine particulate matter and secondary particles are the main contributors, while a lower $PM_{2.5}/PM_{10}$ ratio indicates that coarse particulate matter generated by natural processes (such as dust) is dominant (Zha et al., 2021; Li et al., 2020). As shown in Figure 6, when the mass ratio of $PM_{2.5}$ to PM_{10} was less than 0.3, the NF_{MH} and NF_{VV} of accumulation mode particles were low. This indicated that lower hygroscopicity and lower volatility components dominated accumulation mode aerosols when particles from natural sources were dominant in the atmosphere. However, when the ratio of $PM_{2.5}$ to PM_{10} was larger than 0.3, the NF_{MH} and NF_{VV} of accumulation mode particles were larger. This suggested that when fine particles from anthropogenic emissions were dominant in the atmosphere, the accumulation mode particles primarily consisted of higher-hygroscopicity and higher-volatility components. Besides, when the mass ratio of $PM_{2.5}$ to PM_{10} was less than 0.3, the particles for 150-300 nm exhibited a low HGF and high VSF, while when the mass ratio of $PM_{2.5}$ to PM_{10} exceed 0.3, the particles for 150-300 nm showed a high HGF and low VSF. This suggested that the hygroscopicity and volatility of accumulated mode aerosols from natural or anthropogenic sources were different. The discrepancy in the values of HGF and VSF at 300nm under different mass ratios of $PM_{2.5}$ to PM_{10} was more pronounced, indicating that anthropogenic and natural sources had different effects on accumulation mode particles of varying sizes.

https://doi.org/10.5194/egusphere-2025-3796
Preprint. Discussion started: 27 August 2025

3.4 The evolution of aerosol hygroscopicity and volatility during dust period

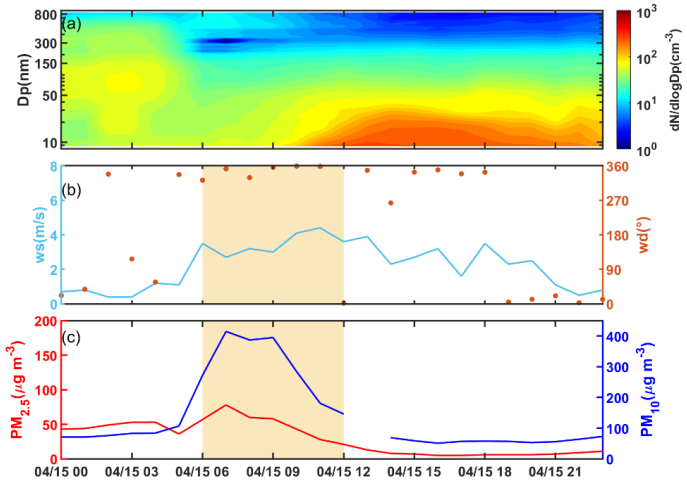

Figure 7. The variation of particle number size distribution, wind speed and wind direction, $PM_{2.5}$ and PM_{10} mass concentration on April 15, 2024. The yellow-shade area represents the dust period.

During the study period, a dust episode was observed on April 15, 2024. In response to this dust event, the Beijing Meteorological Observatory issued a blue dust warning (https://yjglj.beijing.gov.cn/art/2024/4/15/art_2472_674730.html, last access: July 30, 2025). Before 06:00 on April 15, the wind speed was relatively low, with $PM_{2.5}$ levels approximately at 50 μg/m^3. The ratio of $PM_{2.5}$ to PM_{10} was high (~0.6), which indicated that fine particles from anthropogenic emissions dominated. The period from 0:00 to 5:00 on April 15 was defined as the before dust period (before-DS). At 6:00, the wind speed increased, and the wind direction was predominantly North. $PM_{2.5}$ and PM_{10} mass concentrations rose rapidly in response to high wind speed, and reached up to 78 and 415 μg/m^3, respectively. Then the $PM_{2.5}$ and PM_{10} mass concentrations decreased gradually. The average ratio of $PM_{2.5}$ to PM_{10} between 6:00 and 12:00 was 0.16, indicating that the dust particles were dominant. The backward trajectory shows that the air mass between 6:00 and 12:00 mainly originated from the central and western of Mongolia, passing through Inner Mongolia and Hebei province before reaching Beijing. So, the dust period (DS) was defined between 06:00 and 12:00 on April 15. After 12 o

https://doi.org/10.5194/egusphere-2025-3796
Preprint. Discussion started: 27 August 2025

'clock, the mass concentrations of PM_{10} was lower than 100 μg/m^3, and the wind speed also gradually decreased. So, the after-dust period (after-DS) was defined between 13:00 and 23:00 on April 15. Besides, a new particle formation (NPF) event occurred during this period, which is the case with the appearance of the nucleation mode, but without clear growth. As shown in Figure S2, after 12:00, the back trajectories still originated from the north of Beijing and passed through Mongolia, Inner Mongolia, which may still bring the dust particles.

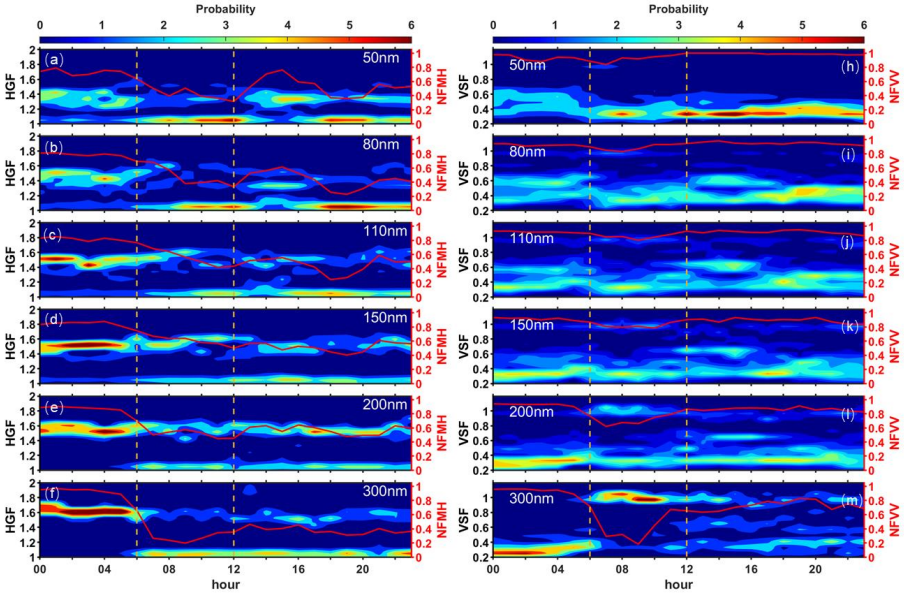

Figure 8. The variation of HGF-PDFs and VSF-PDFs for 50, 80, 110, 150, 200 and 300 nm particles on April 15, 2024. The area between the yellow dashed lines indicates the dust period.

https://doi.org/10.5194/egusphere-2025-3796
Preprint. Discussion started: 27 August 2025

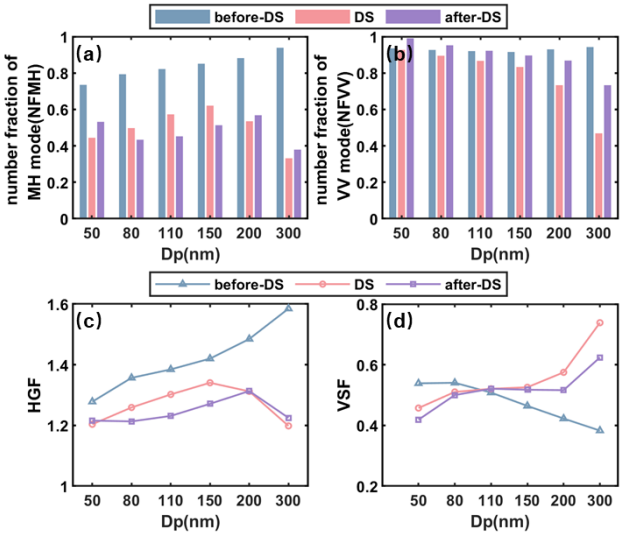

Figure 9. The number fraction of MH mode and VV mode, the mean value of HGF and VSF for 50-300 nm on April 15, 2024.

Figure 8 illustrates the variation of HGF-PDFs and VSF-PDFs for 50, 80, 110, 150, 200, and 300 nm particles on April 15, 2024. Before the dust period, the more hygroscopic mode was more prominent, no matter what particle size was considered. With increasing particle size, the dominance of the more hydroscopic mode became more pronounced. The number fraction of MH mode for 300nm particles was as high as 93.9%. In terms of volatility, the very volatile mode particles for 50-300nm particles were dominant, with the number fraction of VV mode exceeding 80%. As shown in Figure 9, both HGF and VSF were strongly size-dependent before the dust period. As the increase of particle size, HGF increased and VSF decreased, indicating that the volatility and hygroscopicity of smaller aerosols were weaker than those of larger aerosol particles. A similar size dependence of HGF and VSF was also observed at the California-Mexico border (Levy et al., 2014).

During the dust period, the proportion of more hygroscopic mode particles decreased rapidly. When the dust arrived, the strong north wind not only brought dust particles but also swept pre-existing fine particulate matter in the atmosphere. The most significant decline in the number fraction of MH mode particles was observed at 200

https://doi.org/10.5194/egusphere-2025-3796
Preprint. Discussion started: 27 August 2025

and 300nm. The mean value of the number fraction of MH mode particles for 200 and 300nm was 0.54 and 0.33, which were much lower than that before the dust period. Previous research also found that the number fraction of MH mode particles for 250 and 350 nm was less than 0.5 during the dust event (Kaaden et al., 2009). Simultaneously, the NV mode of 200 and 300 nm became more prominent. During the dust period, the minimum NF_{VV} was only 0.18. The mean value of the number fraction of VV mode for 200 and 300 nm particles decreased from 0.93 and 0.94 before the dust period to 0.73 and 0.47 during the dust period, respectively. The decrease in the number fraction of MH mode and the number fraction of VV mode particles for 200 and 300 nm reflected a shift toward hydrophobic and non-volatile components. Besides, HGF and VSF exhibited different size dependence during the dust period compared with before the dust. During the dust period, HGF reached a peak at 150nm and then declined as the particle size increased (Figure 9c). The mean HGF for 300nm was 1.20, which was close to the observed results of Massling et al. (2007) during the dust period. During the dust period, the VSF for 50nm was the least, and the VSFs for 80-150 nm were close. While VSF increased with the increase of particle size from 150-300 nm, reaching as high as 0.74 at 300nm during the dust period (Figure 9d).

During the after-dust period, the number fraction of MH mode particles for 50-300 nm gradually increased, but remained below that before the dust period. Particularly, the MH modes of 50 nm became strong and the number of MH mode of 50nm gradually increased and reached 0.76 at 3:00 (Figure. 8a). This might be related to the NPF event that occurred after the dust. Zhang et al. (2023) reported that the hygroscopicity of 50 nm particles was usually affected by NPF events. Previous studies demonstrated that a significant enhancement in the hygroscopicity of 40nm organic aerosol particles during NPF(Liu et al., 2021) and an increase in the proportion of water-soluble compounds in newly formed particles(Shantz et al., 2012; Wu et al., 2016). During the evening rush hour, it can be clearly observed that the number fraction of MH mode for 50-110 nm particles decreased markedly, probably owing to fresh traffic and cooking emissions during the evening rush hour (Figure 8a-c). After the dust, the

https://doi.org/10.5194/egusphere-2025-3796
Preprint. Discussion started: 27 August 2025

VV mode of 50nm particles became more pronounced (Figure 8g), which could be related to the volatile matters that produced during the NPF event (Wu et al., 2017). The average VSF at 50nm was 0.41 after the dust, which was close to the VSF at 50nm observed during the NPF event in Wu et al. (2017). Size-dependent variations in HGF and VSF during the after-dust period resembled those during the dust period. After the dust, HGF at 200 and 300nm were 1.31 and 1.22. The VSFs at 200 and 300nm were 0.52 and 0.62, which were lower than those during the dust period.

4. Conclusion

Simultaneous measurements of hygroscopicity and volatility of aerosol were performed using a Volatility-Hygroscopicity Tandem Differential Mobility Analyzer (VH-TDMA) in Beijing during April 2024. Results show that 50 nm particles were dominated by the nearly hydrophobic (NH) mode, which could be related to the particles for 50nm being mainly influenced by local emissions, such as traffic emissions and cooking sources. For 80, 110, 150, 200, and 300 nm particles, the more hygroscopic (MH) mode in the HGF-PDF was basically more dominant. During the study period, the mean HGF values for particles ranging from 50 to 300 nm were 1.20±0.07, 1.28±0.07, 1.32±0.07, 1.36±0.08, 1.40±0.09, and 1.43±0.13, respectively. For 50–300 nm particles, the VSF-PDF was mainly dominated by the very volatile (VV) mode, with mean VSF values during the study period being 0.48±0.05, 0.52±0.04, 0.53±0.05, 0.53±0.06, 0.53±0.07, and 0.54±0.10 for the respective sizes.

Back trajectory analyses indicated that Cluster 2, originating from the northwest, exhibited a smaller HGF and a larger VSF, suggesting that the particles from the northwestern air mass had weak hygroscopicity and weak volatility. This could be due to the fact that Cluster 2 passed through the Gobi Desert during its transport, carrying dust aerosols, which led to a decrease in the aerosol hygroscopicity and volatility. The relationships between the hygroscopicity and volatility of aerosol show that the accumulation mode particles exhibited a significant negative correlation between HGF and VSF, and the correlation became strong with an increase in size. Besides, when the

https://doi.org/10.5194/egusphere-2025-3796
Preprint. Discussion started: 27 August 2025

mass ratio of $PM_{2.5}$ to PM_{10} was less than 0.3, the NF_{MH} and NF_{VV} of accumulated mode particles were low, suggesting that accumulated mode particles were dominated by components with lower hygroscopicity and volatility when particles from natural sources were dominant in the atmosphere. Conversely, when the dominance of fine particles from anthropogenic emissions ($PM_{2.5}/PM_{10}$ >0.3), higher NF_{MH} and NF_{VV} values for accumulation mode particles indicated that they were primarily composed of more hygroscopic and volatile components.

The influence of dust process on the hygroscopicity and volatility of aerosol at different sizes was also investigated. Before the dust period, the more hygroscopic mode was prominent regardless of size. The number fraction of MH mode increased with particle diameter (93.9 % at 300 nm). As for volatility, very volatile (VV) mode was dominant and the number fraction of VV mode for 50-300nm particles was higher than 80%. Both HGF and VSF exhibited a clear size dependence: as the increase of particle size, HGF increased and VSF decreased, indicating that smaller particles were less hygroscopic and less volatile. Compared with before the dust period, the mean MH mode fraction dropped sharply to 0.54 for 200 nm and 0.33 for 300 nm, and the mean VV mode fraction decreased to 0.73 (200 nm) and 0.47 (300 nm) during the dust period. This reflected a shift toward hydrophobic and non-volatile components. During the dust period, HGF reached a peak at 150nm and then declined as the particle size increased. The mean HGF was 1.20 for 300 nm during the dust period. While VSF increased with the increase of particle size from 150 to 300 nm, reaching as high as 0.74 at 300nm. After the dust, the MH mode fraction gradually increased but remained below that before the dust period. An NPF event temporarily elevated the MH mode fraction of 50 nm particles to 0.76, while fresh traffic and cooking emissions reduced it during the evening rush hour. Affected by the NPF event, the VV mode of 50 nm particles was enhanced. After the dust, the size-dependent patterns of HGF and VSF resembled those during the dust period, demonstrating a persistent dust influence. To our knowledge, this work focuses on the dust impact on the hygroscopicity and volatility of fine particles simultaneously in the North China Plain for the first time. The results reveal

https://doi.org/10.5194/egusphere-2025-3796
Preprint. Discussion started: 27 August 2025

that the hygroscopicity and volatility of accumulated mode particles are significantly influenced by dust. Accumulated mode plays a significant role in cloud condensation nuclei (CCN) activation. Further research is needed to quantify the changes in accumulation mode properties influenced by dust, specifically their impact on CCN activation.

Data availability.

The full data are available at https://doi.org/10.5281/zenodo.16957115 (Hu et al., 2025).

Competing interests.

The authors declare that none of the authors has any competing interests.

Author contributions.

XH analyzed the observational data, prepared the figures and wrote the original draft. AY conducted the instrument deployment, measurement and data processing. JS designed the experiment, reviewed and finalized the manuscript. All co-authors discussed the results and commented on the manuscript.

Acknowledgements.

This research was supported by the Innovation Team for Haze-fog Observation and Forecasts of MOST.

Financial support.

This study was supported by the China Meteorological Administration (CXFZ2024J039), the National Key Research and Development Program of China (2023YFC3706305, 2024YFC3712902), the National Natural Science Foundation of China (42475121, 42275121,42075082), Basic Research Fund of CAMS (2025Y002, 2023Z012, 2024Z006). It was also supported by the Innovation Team for Haze-fog Observation and Forecasts of MOST.

https://doi.org/10.5194/egusphere-2025-3796
Preprint. Discussion started: 27 August 2025

References

Adebiyi, A., Kok, J. F., Murray, B. J., Ryder, C. L., Stuut, J.-B. W., Kahn, R. A., Knippertz, P., Formenti, P., Mahowald, N. M., Pérez García-Pando, C., Klose, M., Ansmann, A., Samset, B. H., Ito, A., Balkanski, Y., Di Biagio, C., Romanias, M. N., Huang, Y., and Meng, J.: A review of coarse mineral dust in the Earth system, Aeolian Research, 60, 10.1016/j.aeolia.2022.100849, 2023.

Cai, M., Tan, H., Chan, C. K., Mochida, M., Hatakeyama, S., Kondo, Y., Schurman, M. I., Xu, H., Li, F., Shimada, K., Li, L., Deng, Y., Yai, H., Matsuki, A., Qin, Y., and Zhao, J.: Comparison of Aerosol Hygroscopcity, Volatility, and Chemical Composition between a Suburban Site in the Pearl River Delta Region and a Marine Site in Okinawa, Aerosol and Air Quality Research, 17, 3194-3208, 10.4209/aaqr.2017.01.0020, 2017.

Chen, L., Zhang, F., Collins, D., Ren, J., Liu, J., Jiang, S., and Li, Z.: Characterizing the volatility and mixing state of ambient fine particles in the summer and winter of urban Beijing, Atmospheric Chemistry and Physics, 22, 2293-2307, 10.5194/acp-22-2293-2022, 2022a.

Chen, L., Zhang, F., Zhang, D., Wang, X., Song, W., Liu, J., Ren, J., Jiang, S., Li, X., and Li, Z.: Measurement report: Hygroscopic growth of ambient fine particles measured at five sites in China, Atmospheric Chemistry and Physics, 22, 6773-6786, 10.5194/acp-22-6773-2022, 2022b.

Chen, S., Liu, J., Wang, X., Zhao, S., Chen, J., Qiang, M., Liu, B., Xu, Q., Xia, D., and Chen, F.: Holocene dust storm variations over northern China: transition from a natural forcing to an anthropogenic forcing, Science Bulletin, 66, 2516-2527, 10.1016/j.scib.2021.08.008, 2021.

Cohen, M. D., Stunder, B. J. B., Rolph, G. D., Draxler, R. R., Stein, A. F., and Ngan, F.: NOAA's HYSPLIT Atmospheric Transport and Dispersion Modeling System, Bulletin of the American Meteorological Society, 96, 2059-2077, 10.1175/bams-d-14-00110.1, 2015.

https://doi.org/10.5194/egusphere-2025-3796
Preprint. Discussion started: 27 August 2025

512 Draxler, R. R. and Hess, G. D.: An overview of the HYSPLIT_4 modelling system of
513 trajectories, dispersion, and deposition, Australian Meteorological Magazine, 47,
514 295-308, 1998.
515 Gao, C. Y., Bauer, S. E., Tsigaridis, K., and Im, U.: Global Influence of Organic Aerosol
516 Volatility on Aerosol Microphysical Processes: Composition and Number, Journal
517 of Advances in Modeling Earth Systems, 16, 10.1029/2023ms004185, 2024.
518 Gui, K., Yao, W., Che, H., An, L., Zheng, Y., Li, L., Zhao, H., Zhang, L., Zhong, J.,
519 Wang, Y., and Zhang, X.: Record-breaking dust loading during two mega dust
520 storm events over northern China in March 2021: aerosol optical and radiative
521 properties and meteorological drivers, Atmospheric Chemistry and Physics, 22,
522 7905-7932, 10.5194/acp-22-7905-2022, 2022.
523 Gui, K., Che, H., Yao, W., Zheng, Y., Li, L., An, L., Wang, H., Wang, Y., Wang, Z., Ren,
524 H. L., Sun, J., Li, J., and Zhang, X.: Quantifying the contribution of local drivers
525 to observed weakening of spring dust storm frequency over northern China (1982-
526 2017), Science of the Total Environment, 894, 164923,
527 10.1016/j.scitotenv.2023.164923, 2023.
528 Gunthe, S. S., King, S. M., Rose, D., Chen, Q., Roldin, P., Farmer, D. K., Jimenez, J.
529 L., Artaxo, P., Andreae, M. O., Martin, S. T., and Pöschl, U.: Cloud condensation
530 nuclei in pristine tropical rainforest air of Amazonia: size-resolved measurements
531 and modeling of atmospheric aerosol composition and CCN activity, Atmospheric
532 Chemistry and Physics, 9, 7551-7575, DOI 10.5194/acp-9-7551-2009, 2009.
533 Gysel, M., McFiggans, G. B., and Coe, H.: Inversion of tandem differential mobility
534 analyser (TDMA) measurements, J Aerosol Sci, 40, 134-151,
535 10.1016/j.jaerosci.2008.07.013, 2009.
536 Hakala, J., Mikkilä, J., Hong, J., Ehn, M., and Petäjä, T.: VH-TDMA: A description and
537 verification of an instrument to measure aerosol particle hygroscopicity and
538 volatility, Aerosol Science and Technology, 51, 97-107,
539 10.1080/02786826.2016.1255712, 2016.
540 Henning, S., Wex, H., Hennig, T., Kiselev, A., Snider, J. R., Rose, D., Dusek, U., Frank,

https://doi.org/10.5194/egusphere-2025-3796
Preprint. Discussion started: 27 August 2025

G. P., Pöschl, U., Kristensson, A., Bilde, M., Tillmann, R., Kiendler-Scharr, A., Mentel, T. F., Walter, S., Schneider, J., Wennrich, C., and Stratmann, F.: Soluble mass, hygroscopic growth, and droplet activation of coated soot particles during LACIS Experiment in November (LExNo), Journal of Geophysical Research: Atmospheres, 115, 10.1029/2009jd012626, 2010.

Hu, X., Sun, J., Xia, C., Shen, X., Zhang, Y., Zhang, X., and Zhang, S.: Simultaneous measurements of PM1 and PM10 aerosol scattering properties and their relationships in urban Beijing: A two-year observation, Science of The Total Environment, 770, 10.1016/j.scitotenv.2021.145215, 2021.

Hu, X., Sun, J., Yu, A., Shen, X., Lu, J., Zhang, Y., Liu, Q., Liu, L., Liang, L., Tong, H., Ma, Q., Zhang, S., Qi, B., Du, R., Che, H., and Zhang, X.: Measurement report: Dust impact on hygroscopicity and volatility of sub micron aerosols: Based on the observation in April of Beijing, Zenodo [D ata set], https://doi.org/10.5281/zenodo.16957115, 2025.

Huffman, J. A., Ziemann, P. J., Jayne, J. T., Worsnop, D. R., and Jimenez, J. L.: Development and Characterization of a Fast-Stepping/Scanning Thermodenuder for Chemically-Resolved Aerosol Volatility Measurements, Aerosol Science and Technology, 42, 395-407, 10.1080/02786820802104981, 2008.

Kaaden, N., Massling, A., Schladitz, A., Müller, T., Kandler, K., Schütz, L., Weinzierl, B., Petzold, A., Tesche, M., Leinert, S., Deutscher, C., Ebert, M., Weinbruch, S., and Wiedensohler, A.: State of mixing, shape factor, number size distribution, and hygroscopic growth of the Saharan anthropogenic and mineral dust aerosol at Tinfou, Morocco, Tellus B: Chemical and Physical Meteorology, 61, 10.1111/j.1600-0889.2008.00388.x, 2009.

Kim, J.-S. and Park, K.: Atmospheric Aging of Asian Dust Particles During Long Range Transport, Aerosol Science and Technology, 46, 913-924, 10.1080/02786826.2012.680984, 2012.

Kok, J. F., Storelvmo, T., Karydis, V. A., Adebiyi, A. A., Mahowald, N. M., Evan, A. T., He, C., and Leung, D. M.: Mineral dust aerosol impacts on global climate and

https://doi.org/10.5194/egusphere-2025-3796
Preprint. Discussion started: 27 August 2025

climate change, Nature Reviews Earth & Environment, 4, 71-86, 10.1038/s43017-022-00379-5, 2023.

Kurai, J., Watanabe, M., Tomita, K., Yamasaki, H. S. A., and Shimizu, E.: Influence of Asian Dust Particles on Immune Adjuvant Effects and Airway Inflammation in Asthma Model Mice, PLoS ONE, 9, 10.1371/journal.pone.0111831, 2014.

Levy, M. E., Zhang, R., Zheng, J., Tan, H., Wang, Y., Molina, L. T., Takahama, S., Russell, L. M., and Li, G.: Measurements of submicron aerosols at the California–Mexico border during the Cal–Mex 2010 field campaign, Atmospheric Environment, 88, 308-319, 10.1016/j.atmosenv.2013.08.062, 2014.

Li, X., Chen, Y., Li, Y., Cai, R., Li, Y., Deng, C., Wu, J., Yan, C., Cheng, H., Liu, Y., Kulmala, M., Hao, J., Smith, J. N., and Jiang, J.: Seasonal variations in composition and sources of atmospheric ultrafine particles in urban Beijing based on near-continuous measurements, Atmospheric Chemistry and Physics, 23, 14801-14812, 10.5194/acp-23-14801-2023, 2023.

Li, Z., Yang, X., Zhao, C., and Fan, T.: Ratio of PM2.5 to PM10 Mass Concentrations in Beijing and Relationships with Pollution from the North China Plain, Asia-Pacific Journal of Atmospheric Sciences, 57, 421-434, 10.1007/s13143-020-00203-4, 2020.

Lian, L., Huang, J., Chen, S., Du, S., Zhang, L., and Yang, J.: A Comprehensive Review of Dust Events: Characteristics, Climate Feedbacks, and Public Health Risks, Current Pollution Reports, 11, 18, 10.1007/s40726-025-00347-9, 2025.

Liu, J., Zhang, F., Ren, J., Chen, L., Zhang, A., Wang, Z., Zou, S., Xu, H., and Yue, X.: The evolution of aerosol mixing state derived from a field campaign in Beijing: implications for particle aging timescales in urban atmospheres, Atmospheric Chemistry and Physics, 25, 5075-5086, 10.5194/acp-25-5075-2025, 2025.

Liu, J., Zhang, F., Xu, W., Sun, Y., Chen, L., Li, S., Ren, J., Hu, B., Wu, H., and Zhang, R.: Hygroscopicity of Organic Aerosols Linked to Formation Mechanisms, Geophysical Research Letters, 48, 10.1029/2020gl091683, 2021.

Lu, J., Shen, X., Ma, Q., Yu, A., Hu, X., Zhang, Y., Liu, Q., Liu, S., Che, H., Zhang, X.,

https://doi.org/10.5194/egusphere-2025-3796
Preprint. Discussion started: 27 August 2025

and Sun, J.: Size-resolved effective density of ambient aerosols measured by an AAC–SMPS tandem system in Beijing, Atmospheric Environment, 318, 10.1016/j.atmosenv.2023.120226, 2024.

Massling, A., Leinert, S., Wiedensohler, A., and Covert, D.: Hygroscopic growth of sub-micrometer and one-micrometer aerosol particles measured during ACE-Asia, Atmospheric Chemistry and Physics, 7, 3249-3259, DOI 10.5194/acp-7-3249-2007, 2007.

Massoli, P., Lambe, A. T., Ahern, A. T., Williams, L. R., Ehn, M., Mikkilä, J., Canagaratna, M. R., Brune, W. H., Onasch, T. B., Jayne, J. T., Petäjä, T., Kulmala, M., Laaksonen, A., Kolb, C. E., Davidovits, P., and Worsnop, D. R.: Relationship between aerosol oxidation level and hygroscopic properties of laboratory generated secondary organic aerosol (SOA) particles, Geophysical Research Letters, 37, 10.1029/2010gl045258, 2010.

McFiggans, G., Artaxo, P., Baltensperger, U., Coe, H., Facchini, M. C., Feingold, G., Fuzzi, S., Gysel, M., Laaksonen, A., Lohmann, U., Mentel, T. F., Murphy, D. M., O'Dowd, C. D., Snider, J. R., and Weingartner, E.: The effect of physical and chemical aerosol properties on warm cloud droplet activation, Atmospheric Chemistry and Physics, 6, 2593-2649, DOI 10.5194/acp-6-2593-2006, 2006.

Pöhlker, M. L., Pöhlker, C., Quaas, J., Mülmenstädt, J., Pozzer, A., Andreae, M. O., Artaxo, P., Block, K., Coe, H., Ervens, B., Gallimore, P., Gaston, C. J., Gunthe, S. S., Henning, S., Herrmann, H., Krüger, O. O., McFiggans, G., Poulain, L., Raj, S. S., Reyes-Villegas, E., Royer, H. M., Walter, D., Wang, Y., and Pöschl, U.: Global organic and inorganic aerosol hygroscopicity and its effect on radiative forcing, Nature Communications, 14, 10.1038/s41467-023-41695-8, 2023.

Pringle, K. J., Tost, H., Pozzer, A., Pöschl, U., and Lelieveld, J.: Global distribution of the effective aerosol hygroscopicity parameter for CCN activation, Atmospheric Chemistry and Physics, 10, 5241-5255, 10.5194/acp-10-5241-2010, 2010.

Querol, X., Alastuey, A., Rodriguez, S., Plana, F., Ruiz, C. R., Cots, N., Massague, G., and Puig, O.: PM10 and PM2.5 source apportionment in the Barcelona

https://doi.org/10.5194/egusphere-2025-3796
Preprint. Discussion started: 27 August 2025

628 Metropolitan area, Catalonia, Spain, Atmospheric Environment 6407–6419, 2001.
629 Rissler, J., Svenningsson, B., Fors, E. O., Bilde, M., and Swietlicki, E.: An evaluation
630 and comparison of cloud condensation nucleus activity models: Predicting particle
631 critical saturation from growth at subsaturation, Journal of Geophysical Research:
632 Atmospheres, 115, 10.1029/2010jd014391, 2010.
633 Rose, D., Nowak, A., Achtert, P., Wiedensohler, A., Hu, M., Shao, M., Zhang, Y.,
634 Andreae, M. O., and Pöschl, U.: Cloud condensation nuclei in polluted air and
635 biomass burning smoke near the mega-city Guangzhou, China - Part 1: Size-
636 resolved measurements and implications for the modeling of aerosol particle
637 hygroscopicity and CCN activity, Atmospheric Chemistry and Physics, 10, 3365-
638 3383, DOI 10.5194/acp-10-3365-2010, 2010.
639 Shantz, N. C., Pierce, J. R., Chang, R. Y. W., Vlasenko, A., Riipinen, I., Sjostedt, S.,
640 Slowik, J. G., Wiebe, A., Liggio, J., Abbatt, J. P. D., and Leaitch, W. R.: Cloud
641 condensation nuclei droplet growth kinetics of ultrafine particles during
642 anthropogenic nucleation events, Atmospheric Environment, 47, 389-398,
643 10.1016/j.atmosenv.2011.10.049, 2012.
644 Shen, X., Sun, J., Kivekäs, N., Kristensson, A., Zhang, X., Zhang, Y., Zhang, L., Fan,
645 R., Qi, X., Ma, Q., and Zhou, H.: Spatial distribution and occurrence probability
646 of regional new particle formation events in eastern China, Atmospheric
647 Chemistry and Physics, 18, 587-599, 10.5194/acp-18-587-2018, 2018.
648 Shi, J., Hong, J., Ma, N., Luo, Q., He, Y., Xu, H., Tan, H., Wang, Q., Tao, J., Zhou, Y.,
649 Han, S., Peng, L., Xie, L., Zhou, G., Xu, W., Sun, Y., Cheng, Y., and Su, H.:
650 Measurement report: On the difference in aerosol hygroscopicity between high
651 and low relative humidity conditions in the North China Plain, Atmospheric
652 Chemistry and Physics, 22, 4599-4613, 10.5194/acp-22-4599-2022, 2022.
653 Tang, M., Huang, X., Lu, K., Ge, M., Li, Y., Cheng, P., Zhu, T., Ding, A., Zhang, Y.,
654 Gligorovski, S., Song, W., Ding, X., Bi, X., and Wang, X.: Heterogeneous
655 reactions of mineral dust aerosol: implications for tropospheric oxidation capacity,
656 Atmospheric Chemistry and Physics, 17, 11727-11777, 10.5194/acp-17-11727-

https://doi.org/10.5194/egusphere-2025-3796
Preprint. Discussion started: 27 August 2025

2017, 2017.

Wang, Y., Zhang, F., Li, Z., Tan, H., Xu, H., Ren, J., Zhao, J., Du, W., and Sun, Y.: Enhanced hydrophobicity and volatility of submicron aerosols under severe emission control conditions in Beijing, Atmospheric Chemistry and Physics, 17, 5239-5251, 10.5194/acp-17-5239-2017, 2017.

Wu, Z. J., Zheng, J., Shang, D. J., Du, Z. F., Wu, Y. S., Zeng, L. M., Wiedensohler, A., and Hu, M.: Particle hygroscopicity and its link to chemical composition in the urban atmosphere of Beijing, China, during summertime, Atmospheric Chemistry and Physics, 16, 1123-1138, 10.5194/acp-16-1123-2016, 2016.

Wu, Z. J., Ma, N., Größ, J., Kecorius, S., Lu, K. D., Shang, D. J., Wang, Y., Wu, Y. S., Zeng, L. M., Hu, M., Wiedensohler, A., and Zhang, Y. H.: Thermodynamic properties of nanoparticles during new particle formation events in the atmosphere of North China Plain, Atmospheric Research, 188, 55-63, 10.1016/j.atmosres.2017.01.007, 2017.

Xu, W., Kuang, Y., Liang, L., He, Y., Cheng, H., Bian, Y., Tao, J., Zhang, G., Zhao, P., Ma, N., Zhao, H., Zhou, G., Su, H., Cheng, Y., Xu, X., Shao, M., and Sun, Y.: Dust-Dominated Coarse Particles as a Medium for Rapid Secondary Organic and Inorganic Aerosol Formation in Highly Polluted Air, Environmental Science Technology, 54, 15710-15721, 10.1021/acs.est.0c07243, 2020.

Xu, W. Q., Sun, Y. L., Chen, C., Du, W., Han, T. T., Wang, Q. Q., Fu, P. Q., Wang, Z. F., Zhao, X. J., Zhou, L. B., Ji, D. S., Wang, P. C., and Worsnop, D. R.: Aerosol composition, oxidation properties, and sources in Beijing: results from the 2014 Asia-Pacific Economic Cooperation summit study, Atmospheric Chemistry and Physics, 15, 13681-13698, 10.5194/acp-15-13681-2015, 2015.

Yu, A., Shen, X., Ma, Q., Lu, J., Hu, X., Zhang, Y., Liu, Q., Liang, L., Liu, L., Liu, S., Tong, H., Che, H., Zhang, X., and Sun, J.: Size-resolved hygroscopicity and volatility properties of ambient urban aerosol particles measured by a volatility hygroscopicity tandem differential mobility analyzer system in Beijing, Atmospheric Chemistry and Physics, 25, 3389-3412, 10.5194/acp-25-3389-2025,

https://doi.org/10.5194/egusphere-2025-3796
Preprint. Discussion started: 27 August 2025

2025.

Zha, H., Wang, R., Feng, X., An, C., and Qian, J.: Spatial characteristics of the PM2.5/PM10 ratio and its indicative significance regarding air pollution in Hebei Province, China, Environmental Monitoring and Assessment, 193, 10.1007/s10661-021-09258-w, 2021.

Zhang, S., Shen, X., Sun, J., Zhang, Y., Zhang, X., Xia, C., Hu, X., Zhong, J., Wang, J., and Liu, S.: Atmospheric Particle Hygroscopicity and the Influence by Oxidation State of Organic Aerosols in Urban Beijing, Journal of Environmental Sciences, 124, 544-556, 10.1016/j.jes.2021.11.019, 2023.

Zhong, J., Zhang, X., Wang, Y., Sun, J., Shen, X., Xia, C., and Zhang, W.: Attribution of the worse aerosol pollution in March 2018 in Beijing to meteorological variability, Atmospheric Research, 250, 10.1016/j.atmosres.2020.105294, 2021.